Journal Applied Mechanics and Technical Physics, Vol. 37, No. 1, 1996

RIBLET CONTROL OF THE LAMINAR–TURBULENT TRANSITION IN A STATIONARY VORTEX ON AN OBLIQUE AIRFOIL

A. V. Boiko, V. V. Kozlov, V. V. Syzrantsev, and V. A. Shcherbakov

UDC 532.526

1. Introduction. In practice considerable attention is paid to the reduction of drag in vehicles. Over the last two decades noticeable attention has been devoted to small grooves or furrows disposed along the local flow velocity near the wall, called riblets, as a mean for managing a turbulent boundary layer. These devices are of rather simple design, need no additional consumption of energy for operation, and can provide drag reduction by more than 10% in some cases.

It was found that the effect of riblets in turbulent boundary layers depends significantly on their geometrical characteristics. Therefore, usually the characteristic sizes of riblets are expressed in terms of "viscous" length units l^*, which are used in describing turbulent layers [1]: $l^* = \nu/v_0^*$ (ν is the kinematic viscosity and v_0^* is the dynamic velocity on the wall, which is defined in terms of the modulus of local shear stress on the wall τ_0 and the density of the medium ρ as $\sqrt{\tau_0/\rho}$). Hereafter the distance between the furrows and their height expressed in l^* units will be denoted by s^+ and h^+, respectively.

The greatest effect is usually achieved when using V- or U-shaped riblets with the distance between segments is on the order of $h^+ = 20$–30 [2–4], which does not exceed the characteristic thickness of the viscous sublayer. However, the action mechanisms of riblets have not been completely revealed yet (see, for example [5]). It is clear that riblets at the place of their mounting modify the boundary conditions on the wall and the mean flow. A change in the longitudinal profile of mean velocity near the wall can affect the momentum loss thickness and can thus directly lead to a change in the frictional drag. In addition, the properties of flow stability and the intensity of processes in the viscous sublayer can vary, but the mechanism of these changes is practically unknown.

It is assumed in [6, 7] that riblets change the structure of turbulence near the wall and suppress transverse motion in longitudinal vortices, which, as is assumed (see [8]), is one of the main structures of the boundary layer. As a result, the low-velocity liquid flow in the outer part of the boundary layer is decelerated and the momentum exchange between the liquid layers decreases. In [3] separate experimental evidence of the validity of the latter hypothesis is presented. It is noted that no data contradicting the hypothesis have been found yet. However, direct verification of this and other assumptions presents certain difficulties in interpretation of the visualization patterns measurements obtained and under nonstationary conditions of turbulent flow [9].

The data available on the effect of riblets on laminar flows are not extensive. Certain facts were obtained in studying the skin structure of fast sharks. The analysis in [10] shows that in laminar flow areas the skin is rather smooth and acquires a riblet form in places where one would expect the appearance of transition processes and turbulence. Thus, the bionic approach points to the fact that conceivably the ribbing exerts an unfavorable or neutral action on surface drag in laminar flows. Actually, the results of direct numerical calculations with Navier–Stokes equations [11, 12] of flow over riblets in a channel and theoretical analysis of viscous flow near riblets [13] indicate that in an undisturbed laminar flow riblets, as a rule, decrease skin friction but enhance total drag due to the greater flow surface area.

Institute of Theoretical and Applied Mechanics, Siberian Division, Russian Academy of Sciences, Novosibirsk 630090. Translated from Prikladnaya Mekhanika i Tekhnicheskaya Fizika, Vol. 37, No. 1, pp. 82–94, January–February, 1996. Original article submitted February 9, 1995.

Nevertheless, in experiments with a body of revolution [4, 14] for free-stream turbulence intensity $\varepsilon = 0.5\%$ no effect of riblets of size $s^+ \approx h^+ = 2$–25 on the drag in the laminar region was registered, although the authors note the low accuracy of the data obtained in this region. At the same time, maximal drag reduction is noted for the transition region (even greater than for the following turbulent section) with riblets $h^+ \approx s^+ = 10$–15 in size. Furthermore, for the transition zone, as distinct from the turbulent zone the effect was positive for all riblet sizes considered. This fact can probably be explained by retardation of the transition by riblets of the considered sizes, since an appreciable decrease in drag is usually observed precisely during the change of the flow regimes.

In studying the transition in the experiments [15, 16] attention was mostly paid to the site of the transition rather than to the drag. The experiments [15] were conducted at free-stream turbulence intensity $\varepsilon = 0.3\%$ for riblets of size $h^+ \approx s^+ \approx 0.3$–$30$. Riblets covered the model surface, including the transition and turbulent flow regions. Unlike in [4, 14], no favorable effect on the transition was found for riblets oriented along and across the flow. The point of transition determined by the maximum mean- square intensity of pulsations moved upstream or remained unchanged.

In [16] at $\varepsilon = 1.5$–3% riblets covered the entire surface of the plate beginning from the leading edge. It was found that the riblets could either retard or accelerate the transition, depending on the presence of local separation near the stagnation point. With separations, riblets of height $h^+ \approx 15$ shifted the transition point downstream by 20–50%. One can assume that with separations riblets affect a finite-thickness boundary layer, and without separations riblets act as turbulence stimulators near the leading edge. The other contradictions between the experimental results [4, 14–16] on the effect of riblets on the transition region are probably also due to a change in the turbulence transition mechanism in the boundary layer depending on the free-stream turbulence intensity ε and other factors.

In particular, in the experiments [17] with a flat plate at a very low free-stream turbulence ($\varepsilon \approx 0.04\%$) it was shown that riblets of height $h^+ \approx 17$–25 strongly destabilize the amplification of Tollmien–Schlichting waves. This may explain the unfavorable effect of riblets in [15], where they were installed beginning with a Reynolds number Re_{δ^*} close to critical $\mathrm{Re}_{\mathrm{cr}}$ at which the amplification of Tollmien–Schlichting waves begins.

The asymptotic analysis carried out in [18] also indicates that riblets exert a destabilizing action on the evolution of Tollmien–Schlichting waves in a laminar flow but stabilize the longitudinal vortices resulting, for example, from Görtler instability. The latter is also indirectly verified in the model experiments of [19, 20] at $\varepsilon \approx 0.04\%$ for riblets of size $h^+ \approx s^+ = 17$–25, where suppression of the breakdown of Λ-vortices on a flat plate was detected.

With a growth in the free-stream turbulence intensity ε of up to 0.5–1%, along with Tollmien–Schlichting waves, the resultant longitudinal vortex structures, which are probably qualitatively similar to those observed in turbulent flows [21], begin to play a significant role in the transition. At $\varepsilon > 1\%$ these structures become decisive in the turbulence transition, while the role of Tollmien–Schlichting waves is not so obvious [22].

The above experiments were performed in two-dimensional laminar boundary layers. As far as the authors know (see also [6, 14]), similar detailed experiments have not yet been performed for three-dimensional or nonsymmetric laminar flows. Along with this, the results of [23], where a simplified experimental simulation of the flow behavior in a viscous boundary layer with superimposed transverse motion was performed, and the accompanying theoretical analysis show that riblets introduce anisotropy into the medium, shifting the effective beginning of the transverse velocity profile with respect to the longitudinal velocity, which can immediately favor the reduction of momentum exchange between the liquid layers. Thus, the presence of pairs of contrarotating vortices, which is usually assumed in the analysis of the efficiency of riblets in turbulent flows, may be not obligatory, and near-wall transverse motion of the liquid can be caused even by a single longitudinal vortex or a set of co-rotating vortices, which takes place in the cross-flow instability on rotating discs, cones, or oblique airfoils [24].

The instability of an artificial strong solitary vortex with cross-sectional dimension of the order of the thickness of the boundary layer δ was studied in [25, 26]. In these works use was made of an oblique airfoil, which is distinctive in that the greater part of its working surface, except for the region near the leading edge,

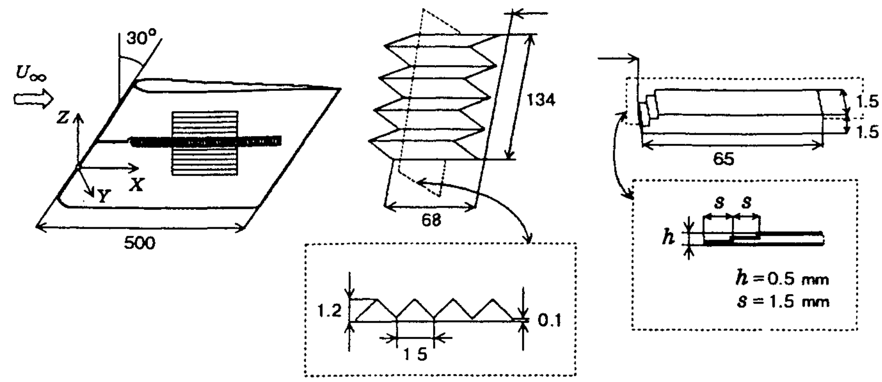

Fig. 1

was a plane surface placed at zero attack angle, which makes this configuration resemble a sliding flat plate. The presence of a plane surface greatly simplifies thermoanemometrical measurements, their processing, and interpretation of the results, as compared with nonplanar surfaces.

The objective of this work is to simulate experimentally the effect of riblets disposed along a stationary vortex described in [25, 26] on the laminar–turbulent transition and the flow structure in the vortex.

2. Experimental Technique. Experiments were performed in a T-324 subsonic low-turbulence closed-type wind tunnel (Institute of Theoretical and Applied Mechanics, Siberian Division, Russian Academy of Sciences) with a sealed test section 1×1 m square and 4 m long. The intensity of turbulence in the test section ε for an experiment does not exceed 0.04% of the approach flow velocity U_∞.

A diagram of the experiment is given in Fig. 1. A C-12 high-lift airfoil [27] with a slip angle of 30° and a chord of 500 mm was selected as the working model. The airfoil was made up of a symmetrical ogive nose with a thickness at the widest part of 16% of the chord and a length of 5.6 cm joined to two identical converging planar surfaces. The profile was situated vertically and secured rigidly to the horizontal walls of the test section so that the working surface of the profile was a flat plane set at a zero angle of attack.

A stationary disturbance evolved behind a projection attached to the surface, whose shape, size, and position on the airfoil are shown in Fig. 1. In order to avoid flow separation on the upstream end of the projection, it was continued to the nonworking side of the airfoil. Its other, downstream end was smoothed.

We used a coordinate system in which the X-axis was directed parallel to the free-stream flow, the Z-axis was directed spanwise to the model and to the side of the transverse flow near the leading edge, and the Y-axis was reckoned from the airfoil surface along the normal to it. The coordinate origin was at an arbitrarily chosen point on the model nose. A coordinate device supporting a hot-wire anemometer probe provided an accuracy of displacement along the airfoil surface of up to 0.5 mm, and from the normal to the airfoil of 0.01 mm. The coordinate $Y = 0$ was determined by linear extrapolation to zero of undisturbed mean-velocity profiles of the laminar boundary layer beyond the vortex with an error of < 0.1 mm.

The free-stream velocity was measured using the difference between the total and static pressures as determined by means of a combined Pitot–Prandtl probe connected to a micromanometer. The basic thermoanemometrical measurements were made in the central part of the model in the range $\Delta Z = 34$ mm where secondary flow is almost absent. Only the longitudinal components of the mean and pulsating flow velocities U and u' were measured. These values were determined by a DISA 55M01 hot-wire anemometer, from which they were fed through an analog-digital converter into a personal computer, where the signals during an experiment were linearized and subjected to spectral analysis, if necessary, using a fast Fourier transform. The signal-linearizing technique is described in [25].

For controlled excitation of traveling waves in the near-wall flow, sound vibrations were transformed into vortex disturbances of the same frequency in a shear layer with local surface nonuniformity. The acoustic vibrations were generated by a dynamic loudspeaker, which was placed behind the model in a tunnel diffuser

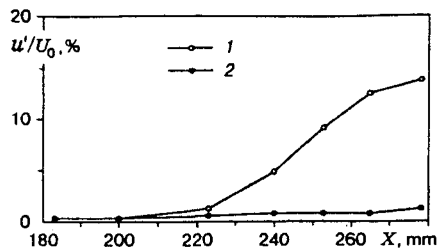

Fig. 2

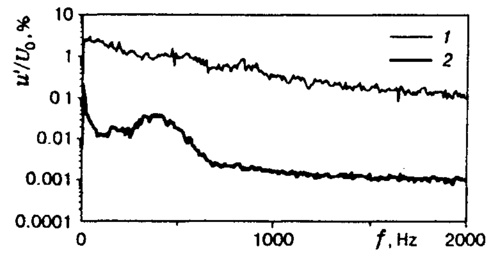

Fig. 3

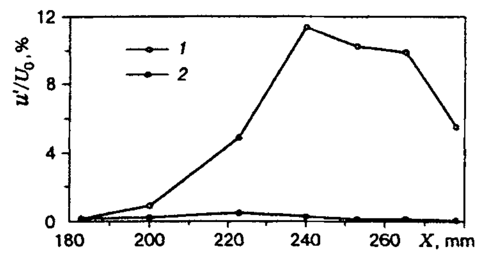

Fig. 4

and emitted sound against the flow direction. The sound frequency and amplitude were set by an audio-signal generator.

It is well known that excitation of sound in the closed space of wind tunnels can produce standing waves which may prevent formation and study of the development of traveling disturbances. However, as special measurements showed, in these experiments the sound amplitude and phase were uniform beyond the boundary layer near the region of generation and evolution of instability waves.

A riblet cover plate of 134 × 68 mm was mounted at a distance of 90 mm from the nearest projection end. This distance was chosen because traveling disturbances are amplified in the vortex at the free-stream velocities being tested beginning from about $X = 90$ mm and one of the objectives of this work is to estimate the effect of riblets on the evolution of these disturbances. The dimensions of the riblet cover plate were much greater than the cross-sectional dimensions of the vortex and separate ribs composing the cover. The riblets were a set of triangular ribs of height $h = 1.2$ mm and base $s = 1.5$ mm made of vulcanized rubber. The back side of the riblets was wetted with water and tightly pressed against the wing surface. Estimates have shown that the thickness of the base and the water layer was of the order of 0.1 mm.

The size and shape of the riblets were not specially optimized in the present experiments, although they were selected based on the following considerations. Up to this point in the present work the riblet sizes were given in "viscous" (internal) length units for the purpose of comparison with the results of other works. For laminar and transitional flows it is considered more natural to normalize by external variables such as the displacement thickness δ^*. Then the riblet heights used in [15, 16, 20] are h = 0.02–0.5, 0.6–1.9, and 1.25–2.0 of δ^*, respectively. Comparison of the results indicates that riblets with a size on the order of the boundary-layer displacement thickness δ^* influence the transition most effectively. In the present work the riblet heights were also on the order of the local value of δ^* (see Section 4) in the region under investigation.

The sensor of the constant-temperature hot-wire probe was a 5-μm tungsten wire placed parallel to the model surface. The filament length was ≈ 0.8 mm, i.e., less than the characteristic sizes of individual ribs, which enabled us to trace their influence on local flow characteristics in the vortex.

The hot-wire probe was calibrated in a free stream opposite the Pitot–Prandtl tube with the flow velocity in the range of 2–10 m/sec, so that the error in determining the mean velocity was less than 1%.

In most cases the distances along the coordinates X, Y, Z and the frequencies are presented in

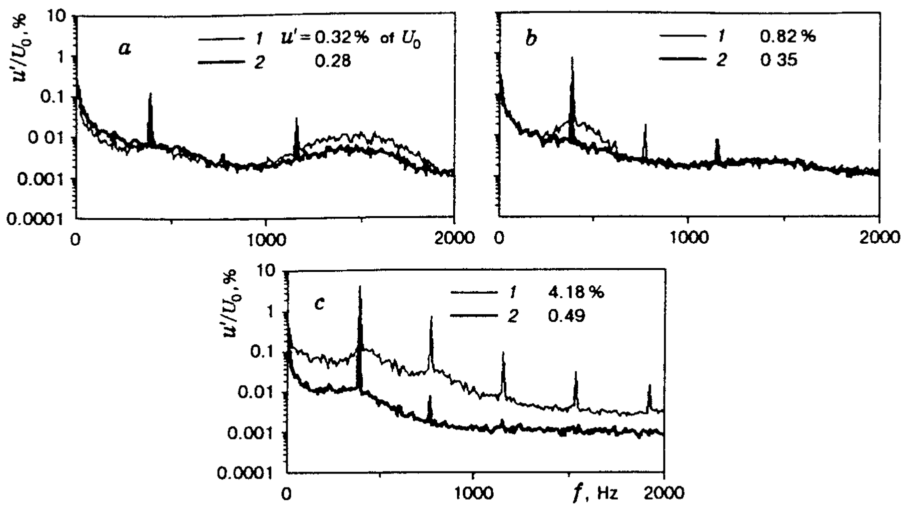

Fig. 5

dimensional form, since in the flow under consideration there are a number of different characteristic parameters (the airfoil chord, the riblet size, the thickness of the boundary layer, the cross-sectional dimension of the vortex, etc.), and at the current stage of research it is far from evident that normalization of any of them is preferable.

3. Observation of the Effect of Riblets on the Evolution of Traveling Disturbances in a Vortex. Figure 2 presents the results of measurement of the integrated (over the spectrum) pulsation intensities u' along the vortex axis in the absence of acoustic excitation of the flow without and with riblets (curves 1 and 2, respectively). The pulsations are given in percentages of the free-stream velocity U_∞ = 7.8 m/sec. The measurements were conducted near the maximum of pulsation intensity in each plane YZ. With a smooth surface the pulsations build up rapidly beginning from the coordinate $X \approx 200$ mm and by the section end achieve $\approx$ 13% of the local velocity of the external flow U_0 at the last point of amplitude measurement. At the same time the level of disturbances over riblets (curve 2) changes insignificantly and reaches 0.8%. As a result the intensities of disturbances in the case under consideration at the end of the measurement section differ by more than an order of magnitude.

The changes occurring over riblets are shown in Fig. 3 by spectra obtained at $X = 278$ mm and the coordinates Y and Z corresponding to Fig. 2. As compared with an undisturbed spectrum (curve 1) over riblets (curve 2) there occurs a strong damping of activity at different frequencies. One can conclude that with the given conditions the flow which was transitional, where gradual filling of the spectrum occurs already at the frequencies f of the order of several kHz, becomes more stationary or laminar with the disturbances concentrated at low frequencies (to 700 Hz).

In [25] the turbulence transition is considered for artificial excitation in a flow of one of the frequency components of a natural wave packet which develops in the vortex. To determine the effectiveness of riblets in this case, the frequency $f_0 = 420$ Hz was chosen, which is close to the frequency with maximum amplification in the natural packet. The downstream behavior of the mean square disturbance intensities in the frequency band of 4 Hz in a flow excited by sound at frequency $f_0 = 420$ Hz is shown in Fig. 4. The measurements were performed near the maximum of the disturbance intensity, i.e., as for the data presented in Fig. 2. Figure 4 shows the faster growth of the disturbances being excited and the turbulence transition for a smooth surface (curve 1), which is registered by the attainment of the pulsation maximum at the coordinate $X = 240$ mm. In the flow with riblets (curve 2) pulsations do not exceed 0.5% of U_∞ and are damped beginning from the coordinate $X \approx 220$ mm. As a result, in this case the riblets diminish the level of pulsations by a factor of tens and lead to flow laminarization in the region where the turbulence transition is observed in the vortex

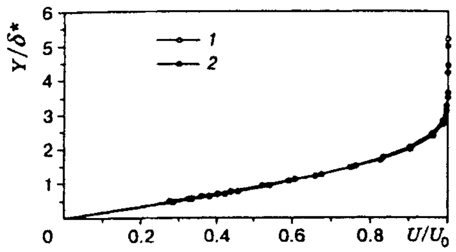

Fig. 6

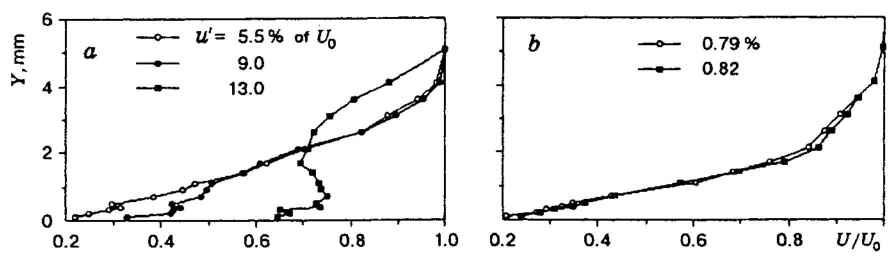

Fig. 7

over a smooth plate.

Figure 5 shows the spectra registered in the vortex at $X = 183$ (a), 200 (b), and 223 mm (c) without (curve 1) and with riblets (curve 2) in a flow excited by sound at frequency $f_0 = 420$ Hz by a technique similar to that used to obtain the data in Figs. 2 and 4. The wave packet of frequencies $f \approx 1100$–1800 Hz, which can be seen in Fig. 5a and was studied in [26], decreases considerably when riblets are present, although the integrated pulsation intensity changes slightly (from 0.32 to 0.28% of U_0). In the next spectrum (Fig. 5b) one can see a decrease in vibration intensity in the region of the low-frequency packet; in this case the integrated vibration intensity at the measurement point decreases from 0.82 to 0.35% of U_0. In the last spectrum the vibration intensity is reduced for practically all frequencies, and the intensity changes integrally from 4.18 to 0.49%. Thus, these riblets in the case being described can essentially decelerate the turbulence transition. Their effect on the vortex is accumulated, i.e., it is the greater, the further downstream from the beginning of the ribbed section the observations are made.

4. Some Mechanisms of the Effect of Riblets on Turbulence Transition in a Vortex. *The Effect of Riblets on the Boundary Layer Surrounding a Vortex.* Figure 6 shows the mean velocity profiles normalized to the local velocity of external flow U_0 as functions of the normal coordinate Y normalized to the displacement thickness δ^*. The profiles are obtained at $X = 278$ mm beyond the vortex without and with riblets; the profile over riblets is shifted by $Y = 0.9$ mm so that the points corresponding to the zero velocity of the profiles coincide. The positions of zero velocity of both profiles are obtained by linear extrapolation of experimental data near the surface. Some characteristics of the boundary layer are found from these profiles by means of integration by the trapezium method.

The momentum loss thicknesses ϑ over riblets and a smooth surface are practically equal: $\vartheta = (0.50 \pm 0.01)$ mm. Along with this, the displacement thickness δ^* changes from (1.26 ± 0.01) mm over a smooth surface to (1.33 ± 0.01) mm over riblets. The local Reynolds number changes in this case from $\mathrm{Re}_{\delta^*} = 655$ to $\mathrm{Re}_{\delta^*} = 692$.

Thus, the riblets cause the mean velocity profile beyond the vortex to be less filled; however, the surface drag, which is proportional to the momentum loss thickness, remains practically unchanged. Theoretically, a less-filled boundary layer profile can facilitate amplification of Tollmien–Schlichting waves in the boundary layer, which is similar to the effect of riblets on a flat plate [17], but this effect was not studied additionally here.

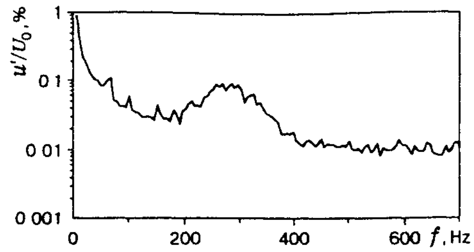

Fig. 8

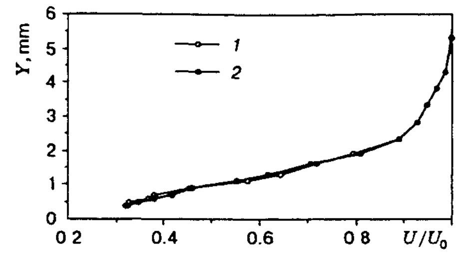

Fig. 9

The Effect of Disturbance Amplitudes on the Mean Characteristics of a Vortex. It was shown in [25] that with motion downstream there is a turbulence transition in a vortex, which is accompanied by a change in the mean velocity distribution in the transverse direction. As the initial intensity of disturbances increases, the transition point is shifted upstream. The change in the mean velocity profile will also move upstream. The task was to select a flow regime such that even strong (severalfold) changes in integrated pulsation amplitudes would not result in distortion of the mean velocity profiles at the end of the measurement region ($X = 278$ mm). The flow was excited at frequency $f_0 = 420$ Hz and the free-stream velocity $U_\infty = 7.8$ m/sec, i.e., at a frequency close to the most-amplified one in this case. It should be noted that frequency-distributed excitation of vibrations would probably give qualitatively similar results, since in exciting a discrete frequency there occurs nonlinear energy redistribution between different frequency components similar to that which takes place in the turbulence transition in other flows (see [28]).

Mean velocity profiles obtained without sound and at two different excitation intensities are shown in Fig. 7a for a smooth surface and in Fig. 7b for riblets. These profiles are registered in the vortex at $X = 278$ mm, when a strong nonlinear wave activity is already observed over a smooth surface. The coordinate Z corresponds to the section in which there is a maximum of pulsation amplitudes in the vortex ($Z = 15$ mm). It is obvious that with a growth in the intensity of integrated vibrations at the measurement point of from $u' = 5.5\%$ to $u' = 9.0\%$ of U_0 the mean velocity profile $U(Y)$ over a smooth surface is first distorted near the wall, and at $u' = 13\%$ is completely rearranged transforming from a filled profile into inflectional profile. In the flow over riblets such changes are not observed; the excitation of a sound level resulting in profile rearrangement in the case without riblets causes only a slight increase in the disturbance intensity at the measurement point of from 0.79 to 0.82% of U_0. Some differences in the profiles for the case with riblets are more likely to be due to inaccurate probe installation along the coordinate Z at the measurement point, where the velocity gradient is great along the coordinate Z rather than to nonlinear waves activity.

Under the given conditions the level of natural disturbances in the vortex on the smooth surface $u' = 5.5\%$ of U_0 is greater than the level over riblets by almost a factor of 7. Then one can assume that a change in the intensity of natural vibrations over riblets can also change the mean velocity distribution in the vortex, i.e., result in recovery of the mean velocity profiles distorted by the nonlinear disturbances activity.

For this reason the free-stream velocity was reduced to $U_\infty = 6.8$ m/sec. The vortex intensity and the growth rate of disturbances in it also decreased. A spectrum registered at $U_\infty = 6.8$ m/sec, $X = 278$ mm over a smooth surface near the maximum of integrated pulsations is shown in Fig. 8. As one could expect (see [25, Fig. 9]), the central frequency of the packet also became smaller and close to 290 Hz. Then at $X = 278$ mm the integrated disturbance intensity on a smooth surface without sound did not exceed 1.3% of U_0, and for sound of great intensity at frequency $f = 290$ Hz it was 2.4% of U_0. The mean velocity profiles corresponding to these regimes are shown in Fig. 9 by curves 1 and 2. Unlike for flow at the free-stream velocity $U_\infty = 7.8$ m/sec, no strong changes in the profiles were observed; therefore, further measurements were taken at $U_\infty = 6.8$ m/sec.

The Effect of Riblets on Flow in a Vortex. It is known that in certain cases the effect of riblets on flow in a vortex can be governed by design features which are not related directly to the presence of ribs. A protrusion on the surface can initiate a pressure gradient and a microseparation of the boundary layer,

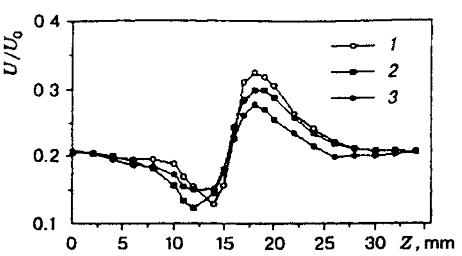

Fig. 10

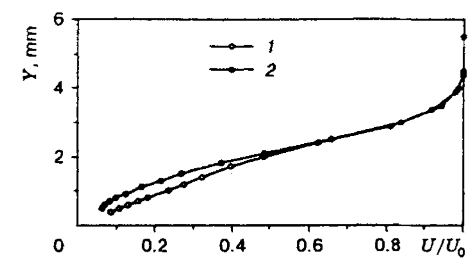

Fig. 11

which can influence strongly the further evolution of the flow. For this reason the data obtained for turbulent flows with riblets and smooth cover plates are often compared (see, for example, [4, 14]). It was also found experimentally in [18, 19] that in a laminar boundary layer on a flat plate a protrusion on the surface produced by riblets changes the fullness of the mean velocity profiles in its vicinity.

When selecting a cover plate the question of its thickness arises, since the displacement due to riblets is nonuniform along the coordinate Z. The average penetration of the mean velocity profile into the furrows between the riblet crests is conventionally called the penetration depth. It was proved theoretically in [3] that for most riblet types this depth does not exceed about 25% of the distance between the ribs. In our case this amounts to ≈ 0.37 mm. Then, the average riblet thickness can be estimated to be 0.83 mm (without the base of thickness ≈ 0.1 mm to which the ribs are secured). Experimental tests based on the extrapolation of mean velocity profiles near the surface of riblets outside the vortex also gave a total thickness on the order of (0.9 ± 0.1)mm (see the above discussion of Fig. 6). Nevertheless, a thicker smooth cover plate of 1.2 mm was used subsequently.

Figure 10 presents the mean velocity distributions in a vortex along the transversal coordinate Z taken at $U/U_0 = 0.21$ (beyond the vortex) over a smooth airfoil surface, over a smooth cover plate, and over a ribbed cover plate (curves 1–3 respectively). It is evident that while over the smooth surface in the given section the difference between the maximum and minimum mean velocity $\Delta U = 21\%$ of the local velocity of the external flow U_0, then over the smooth cover plate $\Delta U = 17\%$ and over riblets $\Delta U = 13\%$.

The measurements were carried out for different U/U_0 and gave qualitatively similar results. Since the effective thickness of the smooth cover plate is approximately by a factor of 1.25 greater than that of riblets, the change in the velocity distribution over riblets can only partially be explained by the action of the protrusion. The remaining differences can be due to the fact that the boundary conditions for smooth and riblet protrusions differ, which can result in a difference in mean velocity distributions immediately behind the protrusion. In addition, as mentioned in Section 3, riblets affect the vortex along its entire length, resulting in smooth variation (along X) of the pulsation amplitudes. One can assume that such a distributed action of riblets will also result in smooth variation of the mean velocity profiles downstream. The following test confirms that both effects took place in the case in question.

It is seen from Fig. 10 that the flow near the minimum and maximum of the mean velocity distribution along Z is subject to the most dramatic changes. Figures 11 and 12 (for $X = 190$ and 278 mm, respectively) show the velocity profiles registered over a smooth surface and riblets (curves 1 and 2) near the distribution minimum ($Z = 12.5$ mm), where the low-velocity medium is carried out into the outer part of the boundary layer. In other words, these profiles are obtained at $X = 190$ mm near the origin of the ribbed section where the effect of the protrusion can manifest itself and far downstream from the protrusion at the section at $X = 278$ mm corresponding to the previous measurements. It is seen from the plots that at $X = 190$ mm the main changes in the profiles occur near the surface and are probably due to the formation of a relaxation region behind the protrusion. At $X = 278$ mm the profile part remote from the surface changes to a greater extent, which can be caused by a change in the momentum exchange between the liquid layers under the effect of riblets.

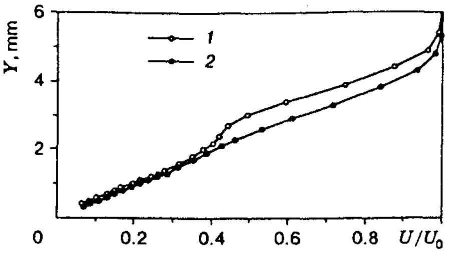

Fig. 12

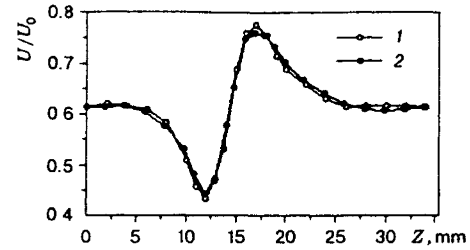

Fig. 13

In all preceding measurements riblets were arranged uniformly so that the positions of their segments coincided. The results of successive measurements of the distributions $U(Z)/U_0$ after a shift of the riblets along Z by half a segment period are shown in Fig. 13. The measurements were performed as the probe moved at height $Y = (1.3 \pm 0.1)$ mm from the effective origin of the riblets or at a height of about 0.9 mm from the rib crests. Even at this distance from the surface, riblet displacement does not result in a distortion of the mean velocity distribution $U(Z)$ exceeding 1%, which is comparable with the measurement accuracy. One can conclude that riblets exert an integrated action independent of the concrete arrangement of the ribs with respect to particular vortex features for most profiles that are separated from the wall. This is in agreement with the results of theoretical analysis in [3], where it was found that at a distance from the rib crests on the order of the distance between the segments the flow becomes practically uniform.

5. Conclusions and Discussion of Results. It was shown in this work that riblets placed on an oblique airfoil can essentially prolong the laminar regime by suppressing the development of nonstationary wave packets that appear in the "natural" turbulence transition in a solitary stationary vortex, as well as the development of artificially excited vibrations in it. The flow over riblets experiences the complex action of the different factors introduced by the riblets. Nonetheless, experimental simulation made it possible to show the principal role of longitudinal furrows in the suppression of vortex motion intensity. Outside the vortex in a laminar boundary layer riblets distort the mean velocity profile, so that the drag remains practically inchanged but thus can contribute to the destabilization of Tollmien–Schlichting waves. The reduced amplification of disturbances in the vortex is only partially explicable by changes in the ambient conditions of the vortex; to a greater degree this decay is due to the change of the vortex itself over riblets.

Further progress in understanding the mechanisms of the effect of riblets can be achieved by varying their characteristics and by a more complete documentation of the structure of the resultant vortex (especially in the near-wall region) by measuring other velocity components in it, as well as modeling vortex generation with roughnesses of other shapes and sizes. The effect of riblets on a periodical system of vortices of this type is far from evident; meanwhile the experiments of [19, 20] show that in certain cases this effect can be rather great.

To date, the effect of pressure gradients on flows over riblets is poorly studied. In the present experiments a protrusion on the surface at the origin of the ribbed section produces a local pressure gradient and definitely influences further development of the flow. The same conclusion on the effect of riblets on the transition for a flat plate can be drawn by analyzing the experimental results of [16], where it is mentioned that depending on the pressure distribution near the leading edge of the plate the effect of riblets can be either positive or negative. The fact that flow separation can be a significant factor determining the effect of riblets in turbulent flows was also mentioned in [5].

It is indicated in [5] with reference to the distributed pressure gradient that for Falkner–Skan parameters β of up to ≈ 0.2, the changes in the effect of riblets in a turbulent boundary layer on a flat plate are insignificant and reduce the drag, at least, to $\beta = 0.5$. When studying the effect of riblets on an inclined body of revolution, it was also found in [4] that in the transition region riblets reduce drag up to attack angles of not less than $\alpha = 7°$. The influence of the distributed pressure gradient on flow in a vortex over riblets was not considered in the experiments and still calls for a separate study.

The authors thank G. R. Grek for technical assistance in the research.

This work was supported by the Russian Foundation for Fundamental Research (Grant 93-13-17359).

REFERENCES

1. H. Schlichting, *Boundary-Layer Theory* [Russian translation], Nauka, Moscow (1969).
2. M. J. Walsh, "Riblets as a viscous drag reduction technique," *AIAA J.*, **21**, No. 4, 485–486 (1983).
3. D. W. Bechert and M. Bartenwerfer, "The viscous flows on surfaces with longitudinal ribs," *J. Fluid Mech.*, **206**, 105–129 (1989).
4. D. Neumann and A. Dinkelacker, "Drag mechanisms on V-grooved surfaces on a body of revolution in axial flow," *Appl. Sci. Res.*, **48**, 101–114 (1991).
5. A. M. Savill, "Drag reduction by passive devices — a review of some recent developments," in: *Structure of Turbulence and Drag Reduction*, A. Gyr (ed.), Springer Verlag, Berlin (1991), pp. 429–465.
6. K. S. Choi, "Drag reduction mechanisms and near-wall turbulence structure with riblets," *ibid.*, pp. 553–560.
7. C. R. Smith, J. D. A. Walker, A. H. Haidari, and B. K. Taylor, "Hairpin vortices in turbulent boundary layers: the implications for reducing surface drag," *ibid.*, pp. 51–58.
8. S. K. Robinson, "A review of vortex structures and associated coherent motions in turbulent boundary layers," *ibid.*, pp. 23–50.
9. M. Kurosaka and P. Sundaram, "Illustrative of stream9lines in unsteady vortices: interpretational differences revised," *Phys. Fluids*, **29**, No. 10, 3474–3477 (1986).
10. A. Dinkelacker, P. Nitscke-Kowsky, and W.-E. Reif, "On the possibility of drag reduction with the help of longitudinal ridges in the walls," in: *Turbulent Management and Relaminarization*, H. W. Liepmann and R. Narasimha (eds.), Springer Verlag, Berlin (1988), pp. 109–120.
11. D. C. Chu, R. Henderson, and G. E. Karniadakis, "Parallel spectral-element-Fourier simulation of turbulent flow over riblet-mounted surfaces," *Theor. Comput. Fluid Dynam.*, **3**, No. 4, 219–229 (1992).
12. D. C. Chu and G. E. Karniadakis, "Direct numerical simulation of a flow over riblets," *J. Fluid Mech.*, **250**, 1–42 (1993).
13. P. Luchini, "Effects of riblets on the growth of laminar and turbulent boundary layers," in: Abstr. of 7th Eur. Drag Reduction Meeting, Sept. 24–25, 1992, Berlin, Germany.
14. M. Schneider and A. Dinkelacker, "Drag reduction by means of surface riblets on an inclined body of revolution," *ibid.*
15. I. A. Belov, G. V. Enyutin, and V. N. Litvinov, "Effect of longitudinal and transverse ribbing of a flat plate on the laminar–turbulent transition," *Uch. Zap. TsAGI*, **21**, No. 6, 107–111 (1990).
16. V. E. Kozlov, V. R. Kuznetsov, B. I. Mineev, and A. N. Secundov, "The influence of free stream turbulence and surface ribbing on the characteristics of a transitional boundary layer," in: *Near-Wall Turbulence*: Proc. of 1988 Zoran Zaric Memorial Conf., S. J. Kline and N. H. Afgan (eds.), Hemisphere Publ. Corp. (1990).
17. G. R. Grek, V. V. Kozlov, and S. V. Titarenko, "An investigation of ribbing of a surface (riblets) on the process of evolution of two-dimensional perturbations (Tollmien–Schlichting waves) in a laminar boundary layer," *Sib. Fiz.-Tekh. Zh.*, No. 6, 26–30 (1993).
18. P. Luchini, "Effects of riblets upon transition," Abstr. of 8th Eur. Drag Reduction Meeting, Sept. 23–24, 1993, Lausanne, Switzerland.
19. G. R. Grek, V. V. Kozlov, and S. V. Titarenko, "An investigation of the effect of surface ribbing on evolution of a solitary wave packet (Λ-vortex) in a laminar boundary layer," *Sib. Fiz.-Tekh. Zh.*, No. 2, 29-36 (1993).

20. G. R. Grek, V. V. Kozlov, and S. V. Titarenko, "An investigation of evolution of a Λ-vortex generated by a blow-suction in a laminar boundary layer at a flat plate and the effect of riblets on it," *Sib. Fiz.-Tekh. Zh.*, No. 6, 31–45 (1993).
21. K. J. A. Westin, A. V. Boiko, B. G. B. Klingmann, et al., "Experiments in a boundary layer subjected to free stream turbulence. Pt I. Boundary layer structure and receptivity," *J. Fluid Mech.*, **281**, 193–218 (1994).
22. A. V. Boiko, K. J. A. Westin, B. G. B. Klingmann, et al., "Experiments in a boundary layer subjected to free stream turbulence. Pt II. The role of TS-waves in the transition process," *J. Fluid Mech.*, **281**, 219–245 (1994).
23. D. W. Bechert and M. Bartenwerfer, "Turbulent drag reduction by nonplanar surfaces — a survey on some recent research at TU/DLR Berlin," in: *Structure of Turbulence and Drag Reduction*, A. Gyr (ed.), Springer Verlag, Berlin (1991), pp. 525–543.
24. Y. Kohama, "Some expectation on the mechanism of cross-flow instability in a swept-wing flow," *Acta Mech.*, **66**, 21–38 (1987).
25. A. V. Boiko, V. V. Kozlov, V. V. Syzrantsev, and V. A. Shcherbakov, "Experimental study of the turbulence transition for a single stationary disturbance in the boundary layer of an oblique airfoil," *Prikl. Mekh. Tekh. Fiz.*, **36**, No. 1, 72–84 (1995).
26. A. V. Boiko, V. V. Kozlov, V. V. Syzrantsev, and V. A. Shcherbakov, "Experimental study of high-frequency secondary perturbations in the boundary layer of an oblique airfoil," *Prikl. Mekh. Tekh. Fiz.*, **36**, No. 3, 74–83 (1995).
27. B. Yu. Zanin and N. V. Lushin, "Comparative studies of a flow around an airfoil in two wind tunnels," *Sib. Fiz.-Tekh. Zh.*, No. 2 (1991).
28. Yu. S. Kachanov, "Physical mechanisms of laminar-boundary-layer transition," *Ann. Rev. Fluid Mech.*, **26**, 411–482 (1994).